# On the impedance response of reactions influenced by mass transfer

Mai Tran Tron Long, Bernard Tribollet, Vincent Vivier, Mark E. Orazem

# On the Impedance Response of Reactions Influenced by Mass Transfer

Mai T.T. Tran,[a] Bernard Tribollet,[a] Vincent Vivier,[a] and Mark E. Orazem[b]

[a] Sorbonne Universités, UPMC Univ Paris 06, CNRS, Laboratoire Interfaces et Systèmes Electrochimiques, 4 place Jussieu, F-75005, Paris, France

[b] Department of Chemical Engineering, University of Florida, Gainesville, FL, 32611, USA

corresponding author: meo@che.ufl.edu

## Abstract

A direct relationship is derived between the charge-transfer resistance and the resistive terms ascribable to diffusion for a faradaic reaction influenced by transport of the reacting species to the electrode. The charge-transfer resistance is shown to approach a finite value for potentials at which the current is limited by mass transfer and, conversely, the diffusion impedance approaches a finite value when the current is controlled by kinetics. Supporting experimental results are presented for both an irreversible (oxygen reduction reaction) and a quasi-reversible electrochemical (ferrocyanide oxidation) systems investigated with a rotating-disk electrode.

**Key Words:** electrochemical impedance spectroscopy; diffusion impedance; rotating disk-electrode; mass-transport limited reaction

# 1. Introduction

Electrochemical impedance spectroscopy is widely used for the elucidation of kinetics of electrochemical processes.[1-3] Following the seminal work of Warburg,[4] who predicted the evolution of the diffusion response in the frequency domain, many authors have attempted to provide a description of diffusion associated with different experimental conditions.[5-6] The diffusion contribution of the impedance was studied for a variety of electrode geometries[7] and using different mathematical approaches.[8] Franceschetti et al. investigated the influence on the diffusion impedance of supporting electrolyte concentration for a reversible redox couple.[9] In the presence of a supporting electrolyte, migration can be neglected, and the mass-transport depends only on diffusion and convection. In general, the calculation of concentration for a convective system is complicated, but in the case of a rotating-disk electrode (RDE), the concentration gradient is constrained inside a thin layer (the so-called Nernst's diffusion layer), in which the mass transport is described by the second Fick's law; whereas, the boundary conditions at the diffusion layer extremities account for the convection.[10]

From an experimental point of view, the Randles circuit[11-12] is commonly used to describe the impedance response for an electrochemical reaction that is influenced by the mass-transport of a reactant to the electrode surface, the latter being described by an analytical expression. This allows expression of the diffusion contribution of the impedance as a function of the potential and the concentration at the electrode surface.

The usual assumption for a faradaic reaction influenced by transport of the reacting species to the electrode is that, at a sufficiently large overpotential, the concentration is null at the interface. Interestingly, the concentration of the reacting species cannot be identically equal to zero at the electrode; the correct assumption is that the concentration at the electrode surface can be neglected when compared to that of the bulk solution.

The corresponding assumptions for the impedance response for a faradaic reaction influenced by transport of the reacting species to the electrode is that the charge-transfer resistance is negligibly small for potentials at which the current is limited by mass transfer and, conversely, the diffusion impedance is negligibly small when the current is controlled by kinetics. The object of the present work is to derive a direct relationship between the charge-transfer resistance and the resistive terms ascribable to diffusion with the single assumption of a finite diffusion-layer thickness. Supporting experimental results are presented for both an irreversible (oxygen reduction reaction) and a quasi-reversible electrochemical (ferrocyanide oxidation) systems investigated with a rotating-disk electrode.

# 2. Mathematical Development

This section presents the development of equations governing steady-state and impedance behavior of faradaic reactions influenced by mass transfer of reacting species.

## 2.1. Steady State Behavior at a RDE - Koutecky-Levich Relationship

For a general electrochemical reaction

$$\mathrm{Ox} + n\mathrm{e}^{-} \rightleftharpoons \mathrm{Red} \tag{1}$$

the rate of the electrochemical reactions may be limited by the finite rate at which reacting species is carried to the electrode surface. Under the assumption that the cathodic and anodic reactions are first order with respect to species Ox and Red, respectively, the faradaic current density can be written as

$$i_{\mathrm{F}} = K_{\mathrm{a}} c_{\mathrm{Red}}(0)\exp(b_{\mathrm{a}}V) - K_{\mathrm{c}} c_{\mathrm{Ox}}(0)\exp(-b_{\mathrm{c}}V) \tag{2}$$

where $K_{\mathrm{a}}$ and $K_{\mathrm{c}}$ are rate constants, $b_{\mathrm{a}} = (1-\alpha)n\mathrm{F}/\mathrm{R}T$, $b_{\mathrm{c}} = \alpha n\mathrm{F}/\mathrm{R}T$, $c_{\mathrm{i}}(0)$ is the interfacial concentration of species i, $n$ is the number of electrons transferred in accordance with the reaction stoichiometry, F is Faraday's constant, $\alpha$ is the symmetry factor, R is the universal gas constant, $T$ is the absolute temperature, and $V$ is the interfacial potential. For

simplicity, the case of a reduction reaction is considered, and thus equation (2) can be simplified as

$$i_{\mathrm{F}} = -K_{\mathrm{c}} c_{\mathrm{Ox}}(0)\exp(-b_{\mathrm{c}}V) \tag{3}$$

The current density corresponds to the flux density of the reacting species, i.e.,

$$i_F = -nFD_{Ox}\left.\frac{dc_{Ox}}{dy}\right|_{y=0} \tag{4}$$

where $D_{\mathrm{Ox}}$ is the diffusion coefficient of Ox, and $y$ is the normal distance to the electrode surface.

Under the assumption of a linear concentration gradient in the diffusion layer of thickness $\delta_{\mathrm{Ox}}$, and a uniform current distribution at the electrode surface, such as may be found with the use of a RDE, the steady-state current density becomes

$$i_F = -nFD_{Ox}\frac{c_{Ox}(\infty)-c_{Ox}(0)}{\delta_{Ox}} \tag{5}$$

where $c_{\mathrm{Ox}}(\infty)$ is the concentration of Ox in the bulk solution. A formal treatment for determination of the value of $\delta_{\mathrm{Ox}}$ requires solution of the convective-diffusion equations. By eliminating $c_{\mathrm{Ox}}(0)$ from equations (1) and (4), the value of the current density is obtained as

$$\frac{1}{i_F} = \frac{1}{i_{lim}} + \frac{1}{i_k} \tag{6}$$

where

$$i_{lim} = -nFD_{Ox}\frac{c(\infty)}{\delta_{Ox}} \tag{7}$$

is the mass-transfer-limited current density and $i_{\mathrm{k}}$ is the kinetic current based on the bulk concentration, which is given as

$$i_{\mathrm{k}} = -K_{\mathrm{c}} c_{\mathrm{Ox}}(\infty)\exp(-b_{\mathrm{c}}V) \tag{8}$$

Equation (6) is called the Koutecky-Levich equation.[1, 13] The numerical value for the mass-transfer-limited current density requires the knowledge of the bulk concentration and diffusivity of the limiting reactant.

The expression of the interfacial concentration of the Ox species, $c_{\mathrm{Ox}}(0)$, is obtained from equations (3) and (5) as

$$c_{\mathrm{Ox}}(0) = \frac{c_{\mathrm{Ox}}{}^{(\infty)}}{\frac{\delta_{\mathrm{Ox}} K_{\mathrm{c}}}{nFD_{\mathrm{Ox}}}\exp(-b_{\mathrm{c}}V)+1} \tag{9}$$

On the cathodic domain, equation (9) shows that $c_{\mathrm{Ox}}(0)$ tends toward zero as $\exp(-b_{\mathrm{c}}V)$ tends toward infinity.

## 2.2. Impedance

For development of impedance equations, the sinusoidal variation of the current density may be expressed as

$$\tilde{\imath}_{\mathrm{F}} = K_{\mathrm{c}} c_{\mathrm{Ox}}(0)\exp(-b_{\mathrm{c}}V) b_{\mathrm{c}}\tilde{V} - K_{\mathrm{c}}\exp(-b_{\mathrm{c}}V)\tilde{c}_{\mathrm{Ox}}(0) \tag{10}$$

leading to

$$\frac{1}{Z_{\mathrm{F}}} = \frac{\tilde{\imath}_{\mathrm{F}}}{\tilde{V}} = \frac{1}{R_{\mathrm{t}}} - K_{\mathrm{c}}\exp\left(-b_{\mathrm{c}}V\right)\frac{\tilde{c}_{\mathrm{Ox}}(0)}{\tilde{V}} \tag{11}$$

where $R_{\mathrm{t}}$ is the charge-transfer resistance

$$R_{\mathrm{t}} = \frac{1}{K_{\mathrm{c}} c_{\mathrm{Ox}}(0) b_{\mathrm{c}}\exp(-b_{\mathrm{c}}V)} \tag{12}$$

Equation (12) is further used to develop expressions for the charge-transfer resistance and the diffusion impedance.

### 2.2.1. Charge-Transfer Resistance

Introduction of equation (9) to equation (12) yields

$$R_\mathrm{t} = \frac{\frac{\delta_\mathrm{Ox} K_\mathrm{c}}{n\mathrm{F}D_\mathrm{Ox}}\exp(-b_\mathrm{c}V)+1}{K_\mathrm{c}c(\infty)b_\mathrm{c}\exp(-b_\mathrm{c}V)} \tag{13}$$

Equation (13) may be expressed as the sum of two contributions

$$R_\mathrm{t} = R_{\mathrm{t_k}} + R_{\mathrm{t_{lim}}} \tag{14}$$

where

$$R_{\mathrm{t_k}} = \frac{1}{K_\mathrm{c}c(\infty)b_\mathrm{c}\exp(-b_\mathrm{c}V)} = -\frac{1}{b_\mathrm{c}i_\mathrm{k}} \tag{15}$$

and

$$R_{\mathrm{t_{lim}}} = \frac{\delta_\mathrm{Ox}}{n\mathrm{F}D_\mathrm{Ox}c(\infty)b_\mathrm{c}} = -\frac{1}{b_\mathrm{c}i_\mathrm{lim}} \tag{16}$$

Thus,

$$R_\mathrm{t} = \frac{-1}{b_\mathrm{c}}\left(\frac{1}{i_\mathrm{k}} + \frac{1}{i_\mathrm{lim}}\right) \tag{17}$$

The above development shows that the charge-transfer resistance may be expressed in terms of the kinetic and limiting currents defined by the Koutecky-Levich relationship as

$$R_\mathrm{t} = R_{\mathrm{t_{lim}}}\left(1 + \frac{i_\mathrm{lim}}{i_\mathrm{k}}\right) \tag{18}$$

At very negative potentials, $i_\mathrm{k}$ becomes very large, and $R_\mathrm{t}/R_{\mathrm{t_{lim}}}$ approaches unity. This result is counterintuitive and is in stark contrast with the behavior of the charge-transfer resistance for a reaction that does not depend on concentration, for which, the charge-transfer resistance can be expressed as[10]

$$R_\mathrm{t} = \frac{1}{K_\mathrm{c}^* b_\mathrm{c}\exp(-b_\mathrm{c}V)} \tag{19}$$

and approaches zero at very negative potentials. Equation (18) contradicts the usual hypothesis for the impedance response of a mass-transfer controlled reaction that the charge-transfer resistance is negligibly small for potentials at which the current is limited by mass transfer (see, for example, page 96 in reference 2.)

2.2.2. Diffusion Impedance

The value of $R_{\mathrm{t}}$, which tends toward a non-zero value for negative over-potential, also affects the diffusion impedance. Equation (11) may be expressed as

$$Z_{\mathrm{F}} = R_{\mathrm{t}} + R_{\mathrm{t}} \frac{K_{\mathrm{c}} \delta_{\mathrm{Ox}} \exp(-b_{\mathrm{c}} V)}{n\mathrm{F} D_{\mathrm{Ox}}} \frac{\tilde{c}_{\mathrm{Ox}}(0)}{\left.\frac{\mathrm{d}\tilde{c}_{\mathrm{Ox}}}{\mathrm{d}y}\right|_{y=0}} \tag{20}$$

Equation (20) may be expressed in terms of diffusion resistance $R_{\mathrm{d}}$ as

$$Z_{\mathrm{F}} = R_{\mathrm{t}} + R_{\mathrm{d}} \left[ \frac{\tilde{c}_{\mathrm{Ox}}(0)}{\left.\frac{\mathrm{d}\tilde{c}_{\mathrm{Ox}}}{\mathrm{d}y}\right|_{y=0}} \right] \tag{21}$$

where

$$R_{\mathrm{d}} = R_{\mathrm{t}} \frac{K_{\mathrm{c}} \delta_{\mathrm{Ox}} \exp(-b_{\mathrm{c}} V)}{n\mathrm{F} D_{\mathrm{Ox}}} \tag{22}$$

Upon insertion of equation (13)

$$R_{\mathrm{d}} = R_{\mathrm{t_{lim}}} \left( \frac{K_{\mathrm{c}} \delta_{\mathrm{Ox}} \exp(-b_{\mathrm{c}} V)}{n\mathrm{F} D_{\mathrm{Ox}}} + 1 \right) \tag{23}$$

In a manner similar to equation (18) for the charge-transfer resistance, the term $R_{\mathrm{d}}$ may be expressed as a function of the kinetic and limiting currents as

$$R_{\mathrm{d}} = R_{\mathrm{t_{lim}}} \left( 1 + \frac{i_{\mathrm{k}}}{i_{\mathrm{lim}}} \right) \tag{24}$$

At very positive potentials, $i_{\mathrm{k}}$ becomes very small, and the ratio $R_{\mathrm{d}}/R_{\mathrm{t_{lim}}}$ approaches unity.

# 3. Experimental section

The working electrode consisted of an Au rotating-disk electrode (RDE) prepared in the lab from a bare Au wire of 5 mm diameter, laterally insulated with a cataphoretic paint and embedded in an epoxy resin. The surface of the exposed disk was polished with SiC paper

(P2400) and the electrode was cycled in sulfuric acid solution (0.5 M) before each experiment. The reference was a mercury-mercurous sulfate electrode in saturated $K_2SO_4$ solution ($E$= 0.64 V/ENH), and the counter electrodes was a platinum gauze.

All solutions were prepared from analytical grade chemicals in double-distilled water. $K_2SO_4$ (purity > 99%) and $K_4Fe(CN)_6$ 3 $H_20$ (purity > 99.95%) were purchased from Sigma-Aldrich, $H_2SO_4$ (purity >95-98%) was purchased from Fluka, and atmospheric oxygen served as the source of dissolved oxygen used in the reduction reaction. All experiments were performed using a Gamry Reference 600 potentiostat. The current / potential curves were recorded at a scan rate of 5 $mVs^{-1}$. The electrochemical impedance diagrams were obtained in a potentiostatic mode over a 100 kHz – 10 mHz frequency domain, using a 5 or 10 mV perturbation (depending on the applied potential) with 12 points per frequency decade.

# 4. Results and Discussion

## 4.1. Variation of the charge-transfer resistance and the diffusion resistance

Equations (18) and (24) show that the charge-transfer and diffusion resistances are governed by the ratio of the kinetic and limiting current defined by Koutecky-Levich. From equations (7) and (8), this ratio can be expressed as

$$\frac{i_{\mathrm{k}}}{i_{\mathrm{lim}}} = \frac{n\mathrm{F}D_{\mathrm{Ox}}}{K_{\mathrm{c}}\delta_{\mathrm{Ox}}}\exp(b_{\mathrm{c}}V) \tag{25}$$

or

$$\ln\left(\frac{i_{\mathrm{k}}}{i_{\mathrm{lim}}}\right) = b_{\mathrm{c}}V + \ln\left(\frac{n\mathrm{F}D_{\mathrm{Ox}}}{K_{\mathrm{c}}\delta_{\mathrm{Ox}}}\right) \tag{26}$$

Equation (26) allows the scaling of the potential $V$ as a function of the kinetic parameters of the system. Interestingly, it also shows the weighting of the mass-transfer-limited current density and the kinetic current with respect to the total current, which is illustrated in Figure 1. In the cathodic domain, $i_{\mathrm{k}}/i_{\mathrm{lim}}$ increases when $V$ decreases. Moreover, the Koutecky-Levich

relationship (Equation 6) indicates that the inverse of the total current is the sum of the inverses of each contribution. As a results, when $V$ decreases, $i_{\mathrm{F}}$ tends towards $i_{\mathrm{lim}}$.

From equation (6), the normalized current can be expressed as

$$\frac{i_{\mathrm{F}}}{i_{\mathrm{lim}}} = \frac{1}{1+\frac{i_{\mathrm{lim}}}{i_{\mathrm{k}}}} \tag{27}$$

The terms $R_{\mathrm{t}}/R_{\mathrm{t_{lim}}}$ from equation (18) and $R_{\mathrm{d}}/R_{\mathrm{t_{lim}}}$ from equation (24) are presented in Figure 2 as functions of the scaled potential $V_{\mathrm{sc}} = b_{\mathrm{c}}V + \ln\left(\frac{n\mathrm{F}D_{\mathrm{Ox}}}{K_{\mathrm{c}}\delta_{\mathrm{Ox}}}\right)$. The dimensionless current density from equation (27) is also shown. From an experimental point of view, $V_{\mathrm{sc}} = 0$ corresponds to the potential at the half value of the diffusion-limited current, and Figure 2 also shows that this potential corresponds to the transition domain for both $R_{\mathrm{t}}/R_{\mathrm{t_{lim}}}$ and $R_{\mathrm{d}}/R_{\mathrm{t_{lim}}}$ variations.

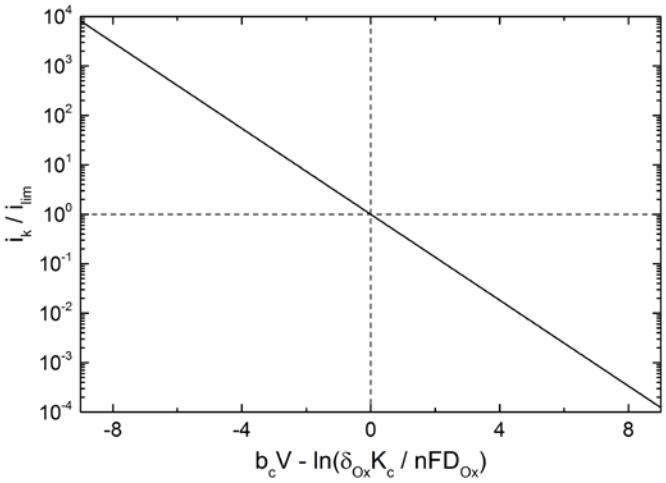


*Figure 1: Evolution of the contribution of the kinetic current based on the bulk concentration to the mass-transfer-limited current as a function of the scaled potential.*

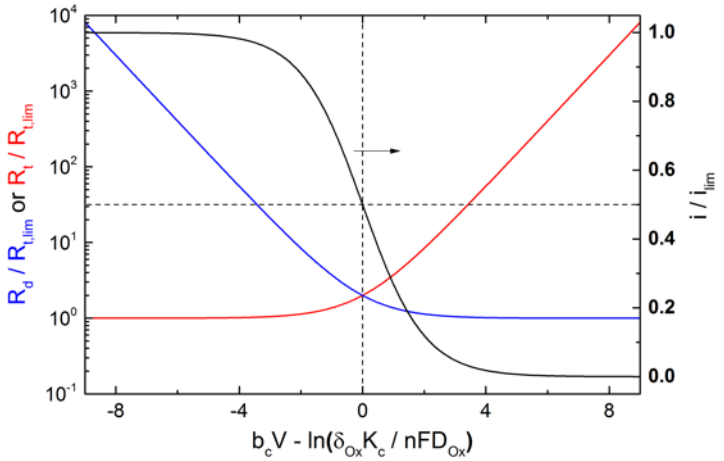


*Figure 2: Evolution of the normalized charge transfer and diffusion resistance (left scale) and normalized current (right scale) as a function of the scaled potential.*

When $V_{sc} < 0$, $R_d/R_{t_{lim}}$ varies linearly with a slope of $-2.303b_c$ and $R_t/R_{t_{lim}} \cong 1$; whereas, when $V_{sc} > 0$, $R_t/R_{t_{lim}}$ varies linearly with a slope of $+2.303b_c$ and $R_d/R_{t_{lim}} \cong 1$. It should also be mentioned that these theoretical curves show that the variations of $R_t/R_{t_{lim}}$ and $R_d/R_{t_{lim}}$ are symmetric with respect to $V_{sc} = 0$.

### 4.2 Irreversible electrochemical reaction

At sufficiently negative potentials, the oxygen reduction reaction (ORR) may be considered to be an irreversible electrochemical system. This reaction is well documented in the literature for various electrode materials and corresponds to an overall 4-electron exchange reaction.[14-15] Numerous investigations report on the influence of the pH on the mechanism, including when experiments are performed at neutral pH.[16-18] In the present work, emphasis is placed on the irreversible process associated with electron transfer. The influence of the rotation rate of the RDE from 30 to 900 rpm is shown in Figure 3a. As expected, for potential lower than -0.9 V/MSE, the reaction rate is governed by diffusion and the current on the plateau varies as the square root of the rotation rate. Additionally, the Koutecky-Levich plot (Figure 3b) shows that

kinetic contribution to the total current (the intercept with the y axis) leads to a current density at the potential of -0.9 V/MSE of about -3.4 $10^{-3}$ A·$cm^{-2}$.

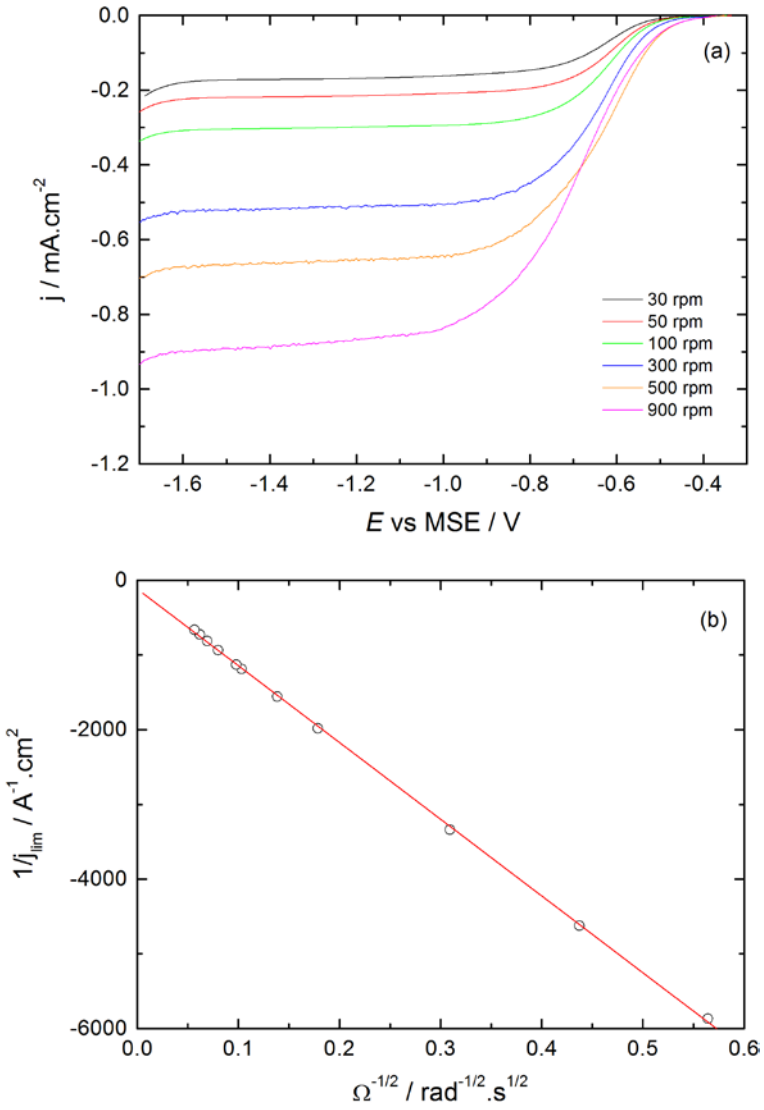


*Figure 3: Oxygen reduction reaction at a gold RDE in 0.1 M $K_2SO_4$ (a) polarization curves as a function of the rotation rate and (b) Koutecky-Levich plot for a potential of -1 V/MSE.*

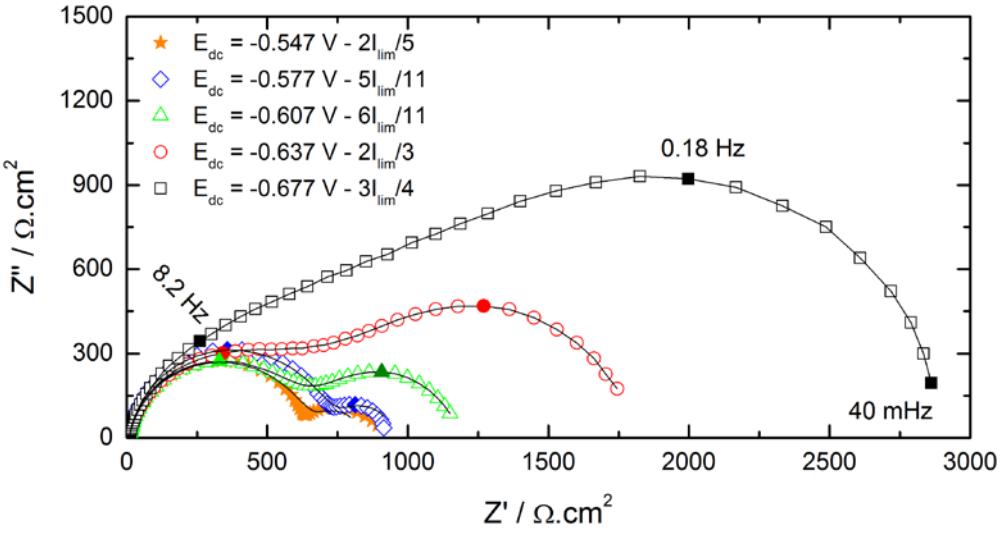


*Figure 4: Nyquist plots of the impedance response at 100 rpm for the ORR on a gold RDE in 0.1 M $K_2SO_4$ with potential as a parameter. Symbols: experimental results; Solid line: fit with the equivalent circuit presented in Figure 5.*

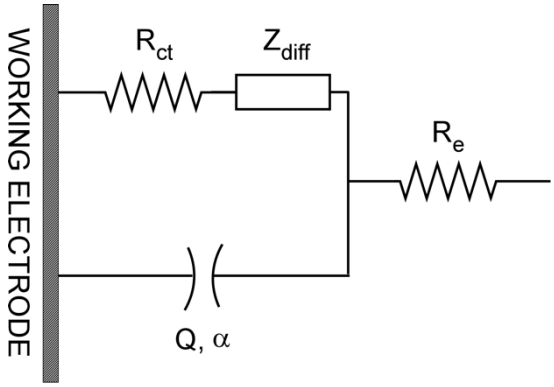


*Figure 5: Electrical equivalent circuit used for fitting the impedance diagrams. $R_e$ is the electrolyte resistance, $R_{ct}$, the charge-transfer resistance, $Z_{diff}$, the diffusion impedance, and Q and $\alpha$ the CPE component accounting for the double-layer capacitance.*

A selection of impedance diagrams are shown in a Nyquist representation in Figures 4. These were measured for the ORR at various potentials before the current plateau at 100 rpm. Similar results were obtained for different rotation rates of the electrode. Two time constants are clearly visible: in the high-frequency domain, the first time constant is associated with the charge-transfer resistance and the double-layer capacitance; whereas, the low frequency time constant can be attributed to the diffusion of electroactive species inside the diffusion layer. These diagrams show that both responses vary as a function of potential. For a potential close to the

value of a diffusion-limited mass transport, the EIS response is dominated by the capacitive behavior of the system, as previously described by Diard and Hecker,[19] and the different contributions may be extracted only by a fine analysis of the response, e.g., by fitting the result with an adequate description of the electrochemical interface.

The equivalent circuit shown in Figure 5 was used for data analysis and fitting. The circuit consists of a Randles equivalent circuit, in which a constant-phase element accounts for the frequency dispersion of the double layer.[20-22] The CPE is in parallel with the charge-transfer resistance and the diffusion impedance. For a better accuracy of the fitting with the experimental data, the CPE was used to account for the double layer relaxation. The values of $\alpha$ ranged from 0.85 to 0.92, and application of the Brug formula[23] yielded double-layer capacitances on the order of 15-25 $\mu F/cm^2$. The diffusion contribution was described according to the analytical expression proposed by Tribollet *et al.*[24-26] for the impedance response of a convective-diffusion equation for a RDE, in agreement with the work of Diard and Montella who compared different numerical methods for the diffusion-convection impedance at a RDE.[27] All of the EIS spectra were fitted as a function of the electrode potential for different rotation rates.

The potential dependence of $R_t$ and $R_d$ obtained from the experiments at 100 and 900 rpm are shown in Figures 6a and 6b, respectively. At 100 rpm (Figure 6a), the asymptotic values of values of $R_t$ and $R_d$ are obviously different, but, from Equations (18) and (24), the ratio of these two quantities may be calculated from the measurement of the mass-transfer-limited current density ($i_{lim}$ = -3 $10^{-4}$ A·$cm^{-2}$) and the kinetic current ($i_k$ = -3.4 $10^{-3}$ A·$cm^{-2}$) determined at E = -1 V/MSE and at -1.2 V/MSE. At a potential of -0.9 V/MSE, $R_t/R_d = 11.3$, in good agreement with the value of 11 obtained from the ratio calculated with the values obtained from the fitting of the EIS diagrams ($R_t$ = 640 Ω·$cm^2$ and $R_d$ = 58 Ω·$cm^2$).

For potential larger than -0.55 V/MSE, the slope of the $R_t$ curve shown in Figure 6a is 6.05 decade/V; whereas, the slope for the $R_d$ curve at potentials smaller than =0.55 V/MSE is -12.2 decade/V. This difference, in absolute value, may be surprising if compared with the result presented in the previous part for a simple electron-exchange reaction showing that both slopes are expected to have equal magnitude. These slopes are indeed an indirect evaluation of the Tafel coefficient and are proportional to the number of electrons exchanged. For the ORR on a gold electrode, the number of electrons exchanged is reported to be 2 for low overpotential (with formation of oxygen peroxide as the reaction product)[13, 28-29]; whereas, the ORR is a 4-electron exchange reaction for large overpotential (with direct formation of water as the reaction product). The ratio of the magnitude of $R_d$ and $R_t$ slopes shown in Figure 6a is 2.02, in agreement with the reported potential dependence for the number of electrons exchanged.

The results obtained at 900 rpm (Figure 6b) are very similar to those previously presented at 100 rpm with a small potential shift (about 80 mV) for the characteristic potential towards the more negative values when the rotation rate increases, that is for a larger current density. A ratio $R_t/R_d = 3.9$ can be determined using the current, which compares favorably with the value of 3.4 obtained from $R_t$ and $R_d$. Interestingly, this value is about 3 times smaller than the value obtained at 100 rpm, which is in agreement with the ratio of the square root of rotation rates. The slope of the $R_t$ and $R_d$ curves as a function of potential are very similar, 6 decade/V and 6.5 decade/V, respectively. These values are in agreement with the slope of 6.05 decade/V obtained for $R_t$ at 100 rpm, which corresponds to a 2-electron charge-transfer reaction. The value of $R_d$ obtained at 900 rpm is close to the value of $R_t$ obtained at 100 rpm. These results indicate that, on this potential range and for this rotation rate (900 rpm), the hydrogen peroxide formed as an intermediate by a two-electron exchange reaction is expelled from the electrode surface due to convection.

The values of $R_t$ and $R_d$ obtained by regression provide a method to extract values for the kinetic current, $i_k$. Equations (18) and (24) yield

$$\frac{R_d}{R_t} = \frac{1 + i_k / i_{lim}}{1 + i_{lim} / i_k} \tag{28}$$

which, as the mass-transfer-limited current density is a constant at a given rotation rate, can be solved for the kinetic current density as

$$i_k = \frac{1}{2}\left( -i_{lim}\left(1 - \frac{R_d}{R_t}\right) - \sqrt{i_{lim}^2\left(1 - \frac{R_d}{R_t}\right)^2 + 4\frac{R_d}{R_t} i_{lim}^2} \right) \tag{29}$$

The results, presented in Figure 7, show that the kinetic current is not a simple exponential function of potential, as would be expected from equation (25). The evolution of a complex mechanism as a function of electrode potential may be followed by use of equation (29), yielding more information than can be obtained by use of the Tafel plot.

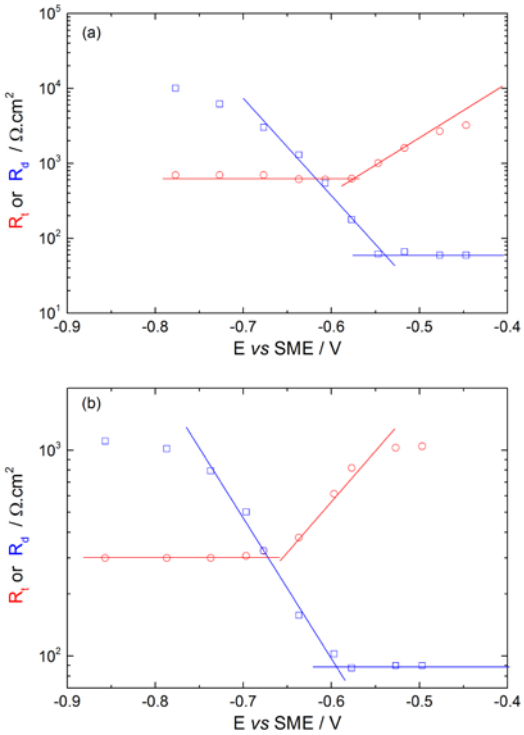


*Figure 6: Experimental values of $R_t$ (red circles) and $R_d$ (blue squares) determined for the ORR (a) 100 rpm and (b) 900 rpm.*

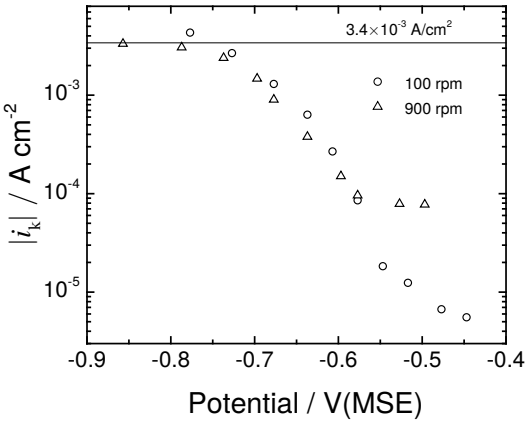


*Figure 7: Experimental values for the kinetic current evaluated from equation (28) for the ORR with rotation rate as a parameter. The value of $3.4\times10^{-3}$ A/cm$^2$ was obtained by extrapolation of the Koutecky-Levich plots, e.g., Figure 3b.*

### 4.3 Quasi-reversible electrochemical reaction

The oxidation of ferrocyanide (10 mM) in $K_2SO_4$ (0.1 M) solution is quasi-reversible with a kinetic constant in the range of $10^{-2}$ to $10^{-3}$ cm·s$^{-1}$, depending on the cleaning procedure of the electrode surface.[30-31] The influence of RDE rotation rate from 30 to 3000 rpm is presented in Figure 8a for the potential range of -0.1 to 1.1 V/MSE. As expected, the shape of the curve is a plateau over a wide potential range (about 900 mV) on which the reaction rate is governed by diffusion, and the current varies as the square root of the rotation rate. The Koutecky-Levich plot (Figure 8b) shows that kinetic current at a potential of 0.6 V/MSE is about 0.13 A·cm$^{-2}$.

Impedance diagrams are presented in Figure 9 in a Nyquist representation for the ferrocyanide oxidation at 900 rpm at different potentials before the current plateau. Similar results were obtained for the different rotation rates of the electrode between 30 to 3000 rpm. The shape of the impedance diagrams corresponds to the simplest case for an electrochemical system involving diffusion: the high-frequency loop attributed to a charge-transfer resistance in parallel with a double-layer capacitance, and effect of diffusion is visible in the lowest frequency domain, corresponding to a diffusion layer of finite thickness. These diagrams were analyzed with the equivalent circuit presented in Figure 5, and the relevant parameters are plotted in Figure 10. Conversely to the previous cases with the ORR, the $R_t$ and $R_d$ curves follow an almost symmetric V-shaped curve. Interestingly, this behavior can be attributed to the quasi-reversibility of the system. The absolute value of the slopes of the curves are 9.5 and 12.5 decade/V for 900 rpm and 100 rpm, respectively. The small difference between the two slopes can be attributed to the value of the apparent transfer coefficient, which differs slightly from 0.5. In that case, for a quasi-reversible system, the two slopes of the V-shaped curves allowed a direct measurement of the apparent transfer coefficient (under the assumption that it is independent of the potential).

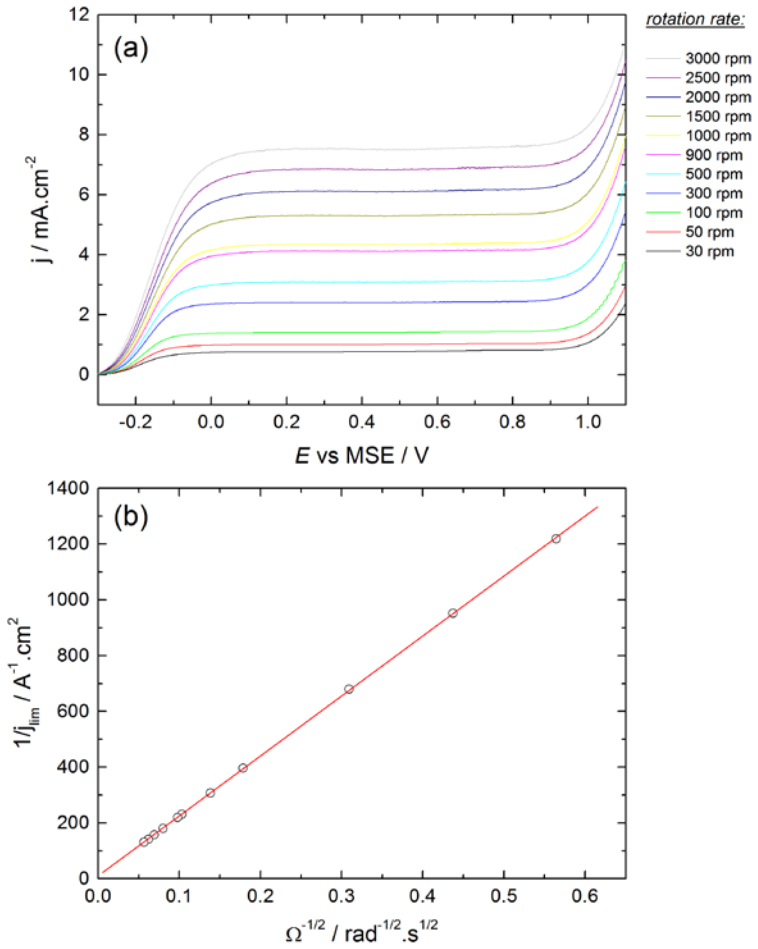


*Figure 8: Ferrocyanide oxidation in 0.1 M $K_2SO_4$ at a gold RDE (a) polarization curves as a function of the rotation rate and (b) Koutecky-Levich plot.*

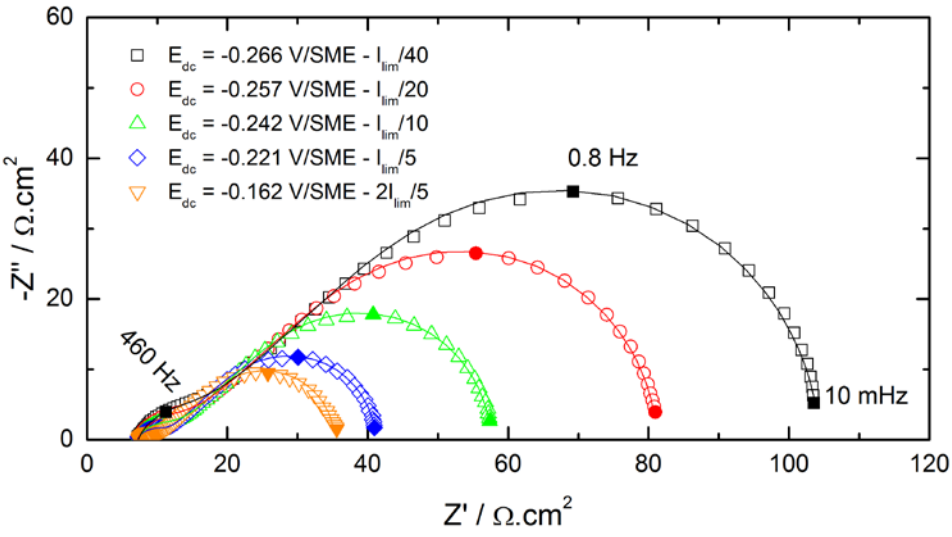


*Figure 9: Nyquist plot of the impedance response for the ferrocyanide oxidation in 0.1 M $K_2SO_4$ at a gold RDE as a function of the potential at 900 rpm – Symbols: experimental results; Solid line: fit with the equivalent circuit presented in Figure 5.*

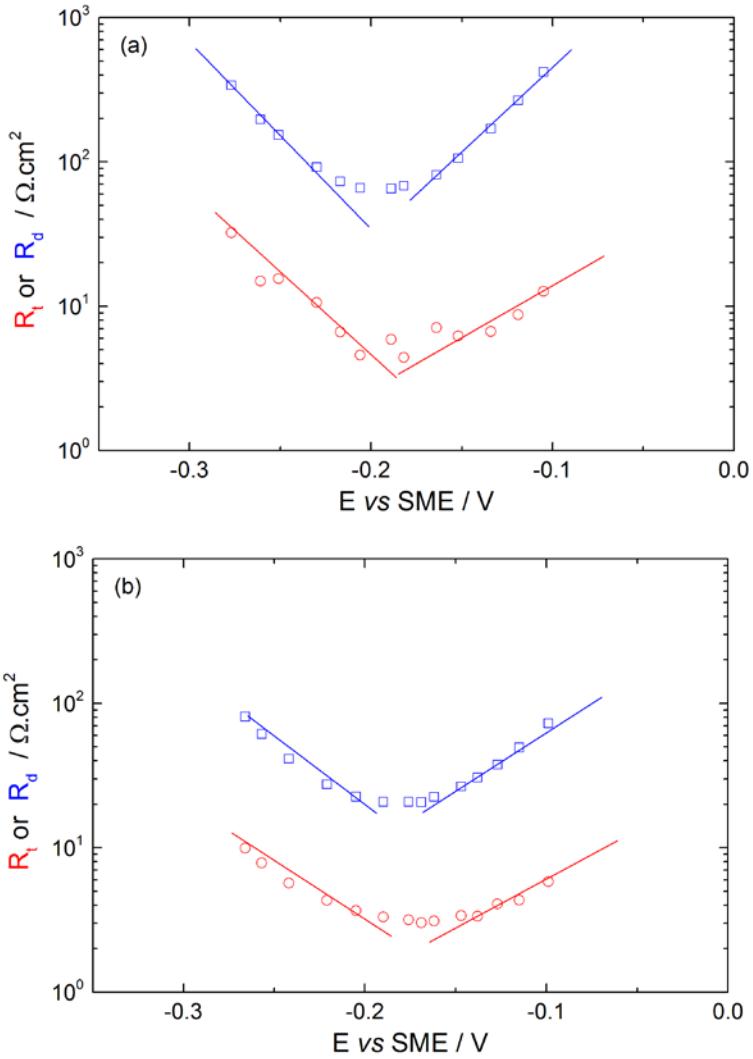


*Figure 10: Experimental values of $R_t$ (red circles) and $R_d$ (blue squares) determined for the ferrocyanide oxidation in 0.1 M $K_2SO_4$ at a gold RDE for (a) 100 rpm and (b) 900 rpm.*

# 5. Conclusions

In the absence of an influence of mass transfer, the charge-transfer resistance associated with an electrochemical reaction tends toward zero as the reaction overpotential tends toward infinity. The present work shows that, for a faradaic reaction influenced by mass transport of a reacting species, the charge-transfer resistance approaches a finite value as the reaction overpotential tends toward infinity (equation (18)), and the current approaches the mass-transport-limited value. Conversely, the diffusion resistance approaches a finite value as the reaction overpotential tends toward zero (equation (24)). For a well-defined reaction with potential-independent values of apparent transfer coefficients, the asymptotic limits for the

charge-transfer and diffusion resistances should be the same (Eq. 26). Differences in these values can be attributed to changes in reaction mechanism as functions of overpotential.

These theoretical developments were supported by experimental results performed for both a reversible redox mediator (the ferri/ferrocyanide couple) and an irreversible electrochemical system (the oxygen reduction reaction). For the latter, it was shown that EIS measurements performed at different potentials allowed investigation of complex mechanisms.

## 6. Acknowledgements

Mark Orazem gratefully acknowledges support from the ExxonMobil Gator Chemical Engineering Alumni and University of Florida Research Foundation Professorships.

Figure Captions

*Figure 1: Evolution of the contribution of the kinetic current based on the bulk concentration to the mass-transfer-limited current as a function of the scaled potential.*

*Figure 2: Evolution of the normalized charge transfer and diffusion resistance (left scale) and normalized current (right scale) as a function of the scaled potential.*

*Figure 3: Oxygen reduction reaction at a gold RDE in 0.1 M $K_2SO_4$ (a) polarization curves as a function of the rotation rate and (b) Koutecky-Levich plot for a potential of -1 V/MSE.*

*Figure 4: Nyquist plots of the impedance response at 100 rpm for the ORR on a gold RDE in 0.1 M $K_2SO_4$ with potential as a parameter. Symbols: experimental results; Solid line: fit with the equivalent circuit presented in Figure 5.*

*Figure 5: Electrical equivalent circuit used for fitting the impedance diagrams. $R_e$ is the electrolyte resistance, $R_{ct}$, the charge-transfer resistance, $Z_{diff}$, the diffusion impedance, and Q and $\alpha$ the CPE component accounting for the double-layer capacitance.*

*Figure 6: Experimental values of $R_t$ (red circles) and $R_d$ (blue squares) determined for the ORR (a) 100 rpm and (b) 900 rpm.*

*Figure 7: Experimental values for the kinetic current evaluated from equation (28) for the ORR with rotation rate as a parameter. The value of $3.4\times10^{-3}$ A/cm$^2$ was obtained by extrapolation of the Koutecky-Levich plots, e.g., Figure 3b.*

*Figure 8: Ferrocyanide oxidation in 0.1 M $K_2SO_4$ at a gold RDE (a) polarization curves as a function of the rotation rate and (b) Koutecky-Levich plot.*

*Figure 9: Nyquist plot of the impedance response for the ferrocyanide oxidation in 0.1 M $K_2SO_4$ at a gold RDE as a function of the potential at 900 rpm – Symbols: experimental results; Solid line: fit with the equivalent circuit presented in Figure 5.*

*Figure 10: Experimental values of $R_t$ (red circles) and $R_d$ (blue squares) determined for the ferrocyanide oxidation in 0.1 M $K_2SO_4$ at a gold RDE for (a) 100 rpm and (b) 900 rpm.*

References


1. Orazem, M. E.; Tribollet, B., In *Electrochemical Impedance Spectroscopy*, John Wiley & Sons, Inc.: 2008; pp 1-525.
2. Lasia, A., In *Electrochemical Impedance Spectroscopy and its Applications*, Springer New York: New York, NY, 2014; pp 1-367.
3. Raistrick, I. D.; Franceschetti, D. R.; Macdonald, J. R., Theory. In *Impedance Spectroscopy*, John Wiley & Sons, Inc.: 2005; pp 27-128.
4. Warburg, E., Polarization capacity of platinum. *Ann. Phys.-Berlin* **1901,** *6* (9), 125-135.
5. Buck, R. P., Diffusion-Migration Impedances for Finite, One-Dimensional Transport in Thin-Layer and Membrane Cells - an Analysis of Derived Electrical Quantities and Equivalent-Circuits. *J. Electroanal. Chem.* **1986,** *210* (1), 1-19.
6. Buck, R. P., Current time responses and impedances of model thin layer and membrane cells with steady state current. *Electrochim. Acta* **1993,** *38* (14), 1837-1845.
7. Jacobsen, T.; West, K., Diffusion impedance in planar, cylindrical and spherical symmetry. *Electrochim. Acta* **1995,** *40* (2), 255-262.
8. Diard, J. P.; Le Gorrec, B.; Montella, C., Linear diffusion impedance. General expression and applications. *J. Electroanal. Chem.* **1999,** *471* (2), 126-131.
9. Franceschetti, D. R.; Macdonald, J. R.; Buck, R. P., Interpretation of Finite-Length-Warburg-Type Impedances in Supported and Unsupported Electrochemical Cells with Kinetically Reversible Electrodes. *J. Electrochem. Soc.* **1991,** *138* (5), 1368-1371.
10. Gabrielli, C., Electrochemical impedance spectroscopy: Principles, Instrumentation, and applications. In *Physical electrochemistry. Principles, methods, and applications*, Rubinstein, I., Ed. Marcel Dekker: New-York, 1995; pp 243-292.
11. Randles, J. E. B., Kinetics of Rapid Electrode Reactions. *Discussions of the Faraday Society* **1947,** *1*, 11-19.
12. Randles, J. E. B.; Somerton, K. W., Kinetics of Rapid Electrode Reactions .3. Electron Exchange Reactions. *Trans. Faraday Soc.* **1952,** *48* (10), 937-950.
13. Bard, A. J.; Faulkner, L. R., *Electrochemical Methods: fundamentals and applications*. second ed.; Wiley-VCH: New-York, 2001.
14. Katsounaros, I.; Cherevko, S.; Zeradjanin, A. R.; Mayrhofer, K. J., Oxygen electrochemistry as a cornerstone for sustainable energy conversion. *Angewandte Chemie* **2014,** *53* (1), 102-21.
15. Jiao, Y.; Zheng, Y.; Jaroniec, M.; Qiao, S. Z., Design of electrocatalysts for oxygen- and hydrogen-involving energy conversion reactions. *Chem Soc Rev* **2015,** *44* (8), 2060-86.
16. Štrbac, S.; Adžić, R. R., The influence of pH on reaction pathways for O2 reduction on the Au(100) face. *Electrochim. Acta* **1996,** *41* (18), 2903-2908.
17. Blizanac, B. B.; Lucas, C. A.; Gallagher, M. E.; Arenz, M.; Ross, P. N.; Marković, N. M., Anion Adsorption, CO Oxidation, and Oxygen Reduction Reaction on a Au(100) Surface: The pH Effect. *J. Phys. Chem. B* **2004,** *108* (2), 625-634.
18. Gotti, G.; Evrard, D.; Fajerwerg, K.; Gros, P., Oxygen reduction reaction features in neutral media on glassy carbon electrode functionalized by chemically prepared gold nanoparticles. *Journal of Solid State Electrochemistry* **2016,** *20* (6), 1539-1550.
19. Diard, J. P.; Hecker, C., Experimental and Theoretical-Study of Impedance Diagram of a Redox System near to the Diffusion Plateau. *J. Electroanal. Chem.* **1981,** *121* (APR), 125-131.

20. Huang, V. M.-W.; Vivier, V.; Orazem, M. E.; Pebere, N.; Tribollet, B., The apparent constant-phase-element behavior of a disk electrode with Faradaic reactions. A global and local impedance analysis. *J. Electrochem. Soc.* **2007,** *154* (2), C99-C107.
21. Huang, V. M.-W.; Vivier, V.; Frateur, I.; Orazem, M. E.; Tribollet, B., The global and local impedance response of a blocking disk electrode with local constant-phase-element behavior. *J. Electrochem. Soc.* **2007,** *154* (2), C89-C98.
22. Huang, V. M.-W.; Vivier, V.; Orazem, M. E.; Pebere, N.; Tribollet, B., The apparent constant-phase-element behavior of an ideally polarized blocking electrode a global and local impedance analysis. *J. Electrochem. Soc.* **2007,** *154* (2), C81-C88.
23. Brug, G. J.; van den Eeden, A. L. G.; Sluyters-Rehbach, M.; Sluyters, J. H., The analysis of electrode impedances complicated by the presence of a constant phase element. *J. Electroanal. Chem.* **1984,** *176* (1-2), 275-295.
24. Deslouis, C.; Gabrielli, C.; Tribollet, B., An Analytical Solution of the Nonsteady Convective Diffusion Equation for Rotating Electrodes. *J. Electrochem. Soc.* **1983,** *130* (10), 2044-2046.
25. Tribollet, B.; Newman, J., Analytic-Expression of the Warburg Impedance for a Rotating-Disk Electrode. *J. Electrochem. Soc.* **1983,** *130* (4), 822-824.
26. Tribollet, B.; Newman, J., The Modulated Flow at a Rotating-Disk Electrode. *J. Electrochem. Soc.* **1983,** *130* (10), 2016-2026.
27. Diard, J. P.; Montella, C., Re-examination of the diffusion–convection impedance for a uniformly accessible rotating disk. Computation and accuracy. *J. Electroanal. Chem.* **2015,** *742*, 37-46.
28. Genshaw, M. A.; Damjanovic, A.; Bockris, J. O. M., Hydrogen peroxide formation in oxygen reduction at gold electrodes: I. Acid solution. *J. Electroanal. Chem.* **1967,** *15*, 163-172.
29. Damjanovic, A.; Genshaw, M. A.; Bockris, J. O. M., Hydrogen peroxide formation in oxygen reduction at gold electrodes: II. Alkaline solution. *J. Electroanal. Chem.* **1967,** *15*, 173-180.
30. Robertson, B.; Tribollet, B.; Deslouis, C., Measurement of Diffusion Coefficients by DC and EHD Electrochemical Methods. *J. Electrochem. Soc.* **1988,** *135* (9), 2279-2284.
31. Gabrielli, C.; Keddam, M.; Portail, N.; Rousseau, P.; Takenouti, H.; Vivier, V., Electrochemical Impedance Spectroscopy Investigations of a Microelectrode Behavior in a Thin-Layer Cell: Experimental and Theoretical Studies. *J. Phys. Chem. B* **2006,** *110* (41), 20478-20485.